Spectral analysis of the sub-tropical percentage data (Fig. 4) indicates coherence with the 23–19-kyr oscillations (precession) just below the 80% confidence interval. The effects of the seasonality and precipitation produced by the increased amplitude of the seasonal cycle of solar radiation appear to have had a significant influence on the distribution and composition of the sub-tropical vegetation in the Hungarian late Pliocene.

The pollen spectrum of both taxonomic groups (that is, boreal and sub-tropical) is, however, dominated by a strong low-frequency component of ~124 kyr. Even though there are only at most three cycles to be resolved in this data set, such variance is clearly visible in the record (Fig. 3). This is of particular significance, as the 124-kyr peak is non-existent in the calculated insolation forcing (Fig. 4)[15].

There is some evidence from oceanic records of significant environmental change at the 95–124-kyr interval. Dust data in deep sea cores exhibit a strong response at this period in the time interval considered here[20]. Changes in atmospheric dust content are thought to reflect directly changes in continental aridity and terrestrial vegetation cover[21], but until now there has been little direct pollen evidence to support this suggestion. The 124-kyr variance observed in our pollen record strongly supports the link between the dust content observed in marine cores and terrestrial vegetation change.

The results from Pula thus indicate that in addition to forcing at the orbital frequencies of precession and obliquity, internally driven nonlinear responses of the climate system at a period of ~124 kyr were as important (if not more important) in driving terrestrial vegetation dynamics and were presumably associated with this broad-scale environmental change. This terrestrial sequence provides the basis for beginning to understand the physical relationships between vegetation, ice volume and insolation forcing during a critical period in the Earth's climate system. □

Received 12 May; accepted 7 December 1998.

1. Shackleton, N. J., Hall, M. A. & Pate, D. *Proc. ODP Sci. Res.* **138,** 337–345 (1995).
2. Maslin, M. A., Haug, G. H., Sarnthein, M. & Tiedemann, R. The progressive intensification of northern hemisphere glaciation as seen from the North Pacific. *Geol. Rundsch.* **85,** 452–465 (1996).
3. Zimmerle, W. in *Paleolimnology of European Maar Lakes* (eds Negendank, J. F. W. & Zolitschka, B.) 1–511 (Springer, Berlin, 1993).
4. Ravasz, C. in *Annual Report of the Hungarian State Geological Instutite for 1974* 221–245 (Hungarian Geol. Inst., Budapest, 1976).
5. Balogh, K. *et al.* in *Annual Report of the Hungarian State Geological Institute for 1980* 243–260 (Hungarian Geol. Inst., Budapest, 1982).
6. Cande, S. C. & Kent, D. V. A new geomagnetic polarity timescale for the Late Cretaceous and Cenozoic. *J. Geophys. Res.* **97,** 13917–13951 (1992).
7. Kukla, G. Loess stratigraphy in central China. *Quat. Sci. Rev.* **6,** 191–219 (1987).
8. Birks, H. J. B. & Gordon, A. D. *Numerical Methods in Quaternary Pollen Analysis* (Academic, London, 1985).
9. Hajós, M. in *Annual Report of the Hungarian State Geological Institute for 1988* 5–13 (Hungarian Geol. Inst., Budapest, 1989).
10. Heinz, T., Rein, B. & Negendank, J. F. W. in *Paleolimnology of European Maar Lakes* (eds Negendank, J. F. W. Zolitschka, B.) 149–161 (Springer, Heidelberg, 1993).
11. van der Hammen, T., Wijimstra, T. A. & Zagwijn, W. H. in *The Late Cenozoic Glacial ages* (ed. Turekian, K. K.) 391–424 (Yale Univ. Press, New Haven, 1971).
12. Tallis, J. H. *Plant Community History. Long-term Changes in Plant Distribution and Diversity* (Chapman & Hall, London, 1991).
13. Suc, J. P. *et al.* Zanclean (Brunssumian) to early Piacenzian (early-middle Reuverian) climate from 4° to 54° north latitude (West Africa, West Europe and West Mediterranean areas). *Meded. Rijks Geol. Dienst* **52,** 43–56 (1995).
14. Jenkins, G. M. & Watts, D. G. *Spectral Analysis and Its Applications* (Holden Day, San Francisco, 1968).
15. Laskar, J., Joutel, F. & Boudin, F. Orbital, precessional and insolation quantities for the Earth from 20 Myr to 10 Myr. *Astron. Astrophys.* **270,** 522–533 (1993).
16. Aitchinson, J. & Brown, J. A. C. *The Lognomial Distribution* (Cambridge Univ. Press, 1969).
17. Tiedemann, R., Sarnthein, M. & Shackleton, N. J. Astronomic timescale for the Pliocene Atlantic $\delta^{18}O$ and dust records of Ocean Drilling Program Site 659. *Paleoceanography* **9,** 619–638 (1994).
18. Thiede, J. & Myhre, A. M. *Proc. ODP Sci. Res.* (eds Thiede, J., Myhre, A. M., Firth, J. V., Johnson, G. L. & Ruddiman, W. F.) 645–659 (1996).
19. Cronin, T. M., Raymo, M. E. & Kyle, K. P. Pliocene (3.2–2.4 Ma) ostracode faunal cycles and deep ocean circulation, North Atlantic Ocean. *Geology* **24,** 695–698 (1996).
20. Tiedemann, R., Sarnthein, M. & Shackleton, N. J. Astronomic timescale for the Pliocene Atlantic ^{18}O and dust flux records of Ocean Drilling Program site 659. *Paleoceanography* **9,** 619–638 (1994).
21. Rea, D. K. The paleoclimatic record provided by eolian deposition in the deep sea: the geologic history of wind. *Rev. Geophys.* **32,** 159–195 (1994).

Acknowledgements. We thank K. D. Bennett, S. Clemens, M. Chapman, C. A. G. Gilligan, C. Heusser, M. F. Loutre, J. C. Ritchie, N. J. S. Shackleton and L. P. Zhou for comments and discussions on this manuscript, and B. Goddard for help with the figures. This work was funded by a Royal Society University Research Fellowship (K.W.) and a King's College Senior Research Fellowship (A.K.).

Correspondence and requests for materials should be addressed to K.J.W. (e-mail: kathy.willis@geog.ox.ac.uk).

Relative impacts of human-induced climate change and natural climate variability

Mike Hulme*, Elaine M. Barrow*, Nigel W. Arnell†, Paula A. Harrison‡, Timothy C. Johns§ & Thomas E. Downing‡

* *Climatic Research Unit, School of Environmental Sciences, University of East Anglia, Norwich NR4 7TJ, UK*
† *Department of Geography, University of Southampton, Southampton SO17 1BJ, UK*
‡ *Environmental Change Unit, University of Oxford, Oxford OX1 3TB, UK*
§ *Hadley Centre for Climate Prediction and Research, The UK Meteorological Office, London Road, Bracknell RG12 2SY, UK*

Assessments of the regional impacts of human-induced climate change on a wide range of social and environmental systems are fundamental for determining the appropriate policy responses to climate change[1–3]. Yet regional-scale impact assessments are fraught with difficulties, such as the uncertainties of regional climate-change prediction[4], the specification of appropriate environmental-response models[5], and the interpretation of impact results in the context of future socio-economic and technological change[6]. The effects of such confounding factors on estimates of climate-change impacts have only been poorly explored[3–7]. Here we use results from recent global climate simulations[8] and two environmental response models[9,10] to consider systematically the effects of natural climate variability (30-year timescales) and future climate-change uncertainties on river runoff and agricultural potential in Europe. We find that, for some regions, the impacts of human-induced climate change by 2050 will be undetectable relative to those due to natural multi-decadal climate variability. If misleading assessments of—and inappropriate adaptation strategies to—climate-change impacts are to be avoided, future studies should consider the impacts of natural multi-decadal climate variability alongside those of human-induced climate change.

Most climate-change impact studies follow a conventional methodology[11,12] of simulating an environmental indicator—for example, runoff, crop yield, natural biome—first, under current climate, and then under a scenario of climate change. These

Table 1 Global and European climate changes for HadCM2 simulations.

	*p_{CO_2} (p.p.m.v.)	†$\Delta T_{ANNglobal}$ (°C)	†$\Delta T_{ANNeurope}$ (°C)	†$\Delta P_{DJFeurope}$ (%)	†$\Delta P_{JJAeurope}$ (%)
‡Control	334	±0.30	±0.24	±1.90	±3.64
§GGa–1	515	1.97	2.57	8.48	–0.33
GGa-2	515	1.88	2.50	5.53	–2.25
GGa-3	515	1.93	2.05	9.37	–4.09
GGa-4	515	1.86	2.09	4.27	–3.33
GGa-mean	515	1.91	2.30	6.89	–2.51
§GGd-1	435	1.42	1.70	6.85	–2.18
GGd-2	435	1.31	1.83	2.40	–0.11
GGd-3	435	1.34	1.48	7.79	–1.61
GGd-4	435	1.44	1.89	5.00	-0.27
GGd-mean	435	1.38	1.72	5.49	–1.04

* Actual CO_2 concentrations for GGa and GGd are estimated using the mix of greenhouse gases in, respectively, the IS92a and IS92d emissions scenarios[30], together with the total CO_2-equivalent forcing used in the HadCM2 experiments.
† ANN, annual; DJF, boreal winter; JJA, boreal summer. Climate changes over Europe are calculated for land only.
‡ Control climate numbers are 2σ model estimates of natural variability on 30-year timescales.
§ GGa and GGd are, respectively, greenhouse-gas-only forcing scenarios equivalent to a 1% and 0.5% yr^{-1} increase in CO_2 concentration from 1990 to 2100[9]. Simulations 1 to 4 represent individual simulations in each ensemble, each with the same forcing but with different initial model conditions[17]. GGa and GGd numbers are model-simulated climate changes extracted for the period 2035–64. All changes are expressed with respect to the 1961–90 mean climate.

scenarios typically represent some future period, for example the year 2050, or some future atmospheric condition, for example twice the pre-industrial level of atmospheric CO_2. If the simulation model incorporates non-climate parameters (for example, fertilizer application) then these may also be perturbed to reflect a different future physical or technological environment. The difference between the two simulations is then an estimate of the impact of human-induced climate change, that is, the 'impact signal'.

Much of the work reported by the Intergovernmental Panel on Climate Change[3,7] has followed this approach, and many estimates of climate-change damage functions used in economic analyses rely on these types of results[13–16]. This methodology is extended here by exploring the effects on impact indicators of uncertainty in the baseline climate (that is, natural climate variability inducing 'impact noise') and uncertainty in the climate-change signal. The former is achieved by using multi-century simulations of unforced climate and the latter through the use of ensemble scenario simulations. A climate-change ensemble consists of a number of simulations made with the same climate model and identical external forcing, but with each simulation starting from slightly different initial conditions. Ensemble simulations therefore provide a representation of the 'unpredictability' of the climate system. This approach allows us to interpret simulated climate-change impacts in a probabilistic framework based on signal-to-noise ratios. Two impact indicators for Europe—runoff and water-limited wheat yield—are used to illustrate the method. We focus on changes in the mean, although our approach can also be applied to extreme events and we provide an example of this.

We use results from a recent set of climate-change experiments performed by the UK Hadley Centre with their coupled ocean–atmosphere model (HadCM2[8,17]). These experiments include a long multi-century control simulation and four ensemble simulations, each ensemble being forced with a different anthropogenic forcing scenario. Seven independent 30-year climates were extracted from the first 240 years of the control simulation, along with 30-year climates for the periods 1961–90 and 2035–64 from two of the four ensembles: GGa and GGd. GGa represents a widely used forcing scenario of 1% yr^{-1} growth in CO_2-equivalent concentrations for the next century, while GGd represents a low forcing scenario of 0.5% yr^{-1} growth[17] (see details in Table 1). These extracted model climates—both control and scenario—are converted into mean climate anomalies from the 1961–90 period of the respective model simulations, which are then added to the observed 1961–90 climate. Inter-annual and inter-daily climate variability is assumed to be unchanged in all cases, our concern in this study being to examine the relative impacts of multi-decadal (30-year timescale) climate variability. We treat the climates resulting from the control simulation as describing multi-decadal 'natural climate variability' (although model-simulated rather than observed) and those from the scenario simulations as describing 'climate change' by the year 2050. Other climate models would yield different results to those shown here, and a full range of forcing scenarios would be necessary for a comprehensive analysis of impact uncertainty; we illustrate one important aspect of uncertainty, however, using the selected data. The observed baseline climate data are monthly mean values for the 1961–90 period gridded at a 0.5° latitude/longitude resolution[18]. The model anomalies at a resolution of 2.5° latitude by 3.75° longitude were interpolated to the observed resolution using a gaussian space-filtering routine. More sophisticated 'downscaling' methods exist[19], but were not applied here.

Runoff was simulated at a spatial scale of 0.5° latitude/longitude, using a daily water balance model applied separately in each cell with soil and vegetation parameters derived from spatial databases[9]. The model does not simulate the direct effect of elevated CO_2 concentrations in reducing potential evapotranspiration, as this is assumed to be offset at the catchment scale by increased plant growth. The monthly input data are 'downscaled' to the daily scale, using a stochastic model that generates randomly distributed daily rainfall amounts constrained by the monthly total. The model simulates well the broad pattern of runoff across Europe, and has been used to assess the implications of climate change[9].

There are three findings from the application of the hydrological model with the different climate data sets. First, the spatial patterns of runoff change resulting from climate change are different to those associated with natural climate variability. The climate change scenarios result in a strong north–south gradient of change[9], while the runoff anomalies due to climate variability are less geographically structured. Second, the patterns of runoff change

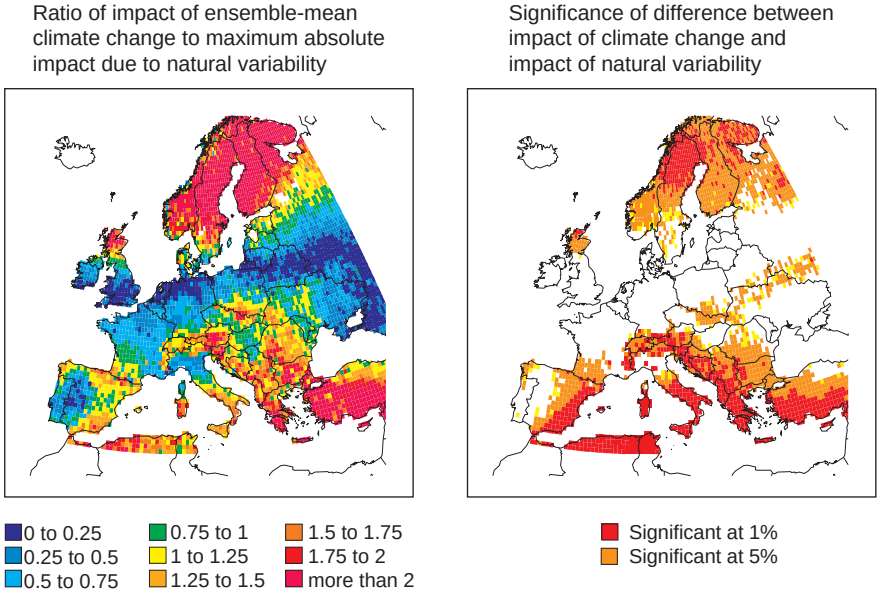

Figure 1 Relative impact of climate change on runoff. Change in mean annual runoff on a grid of 0.5° resolution across Europe due to climate change by 2050 under the GGa forcing scenario, expressed relative to the change in runoff due to natural climate variability. Left panel, absolute ensemble-mean per cent change in mean annual runoff by 2050 expressed as a ratio of the absolute maximum per cent change in annual runoff caused by natural climate variability. Ensemble-mean runoff change is the average of the four runoff changes induced by the four ensemble climate changes. Right panel, significance of the difference in mean annual runoff induced by 2050 climate change (n=4) and by natural climate variability (n=7); two-tailed t-test.

are less consistent between the different natural climates (an average impact pattern correlation amongst the seven experiments of 0.21) than between the climate-change scenarios (average impact pattern correlations of 0.78 and 0.56 for GGa and GGd, respectively, with the lower correlations under GGd reflecting the weaker climate forcing of these simulations). Third, and most important at the catchment and water management scale, the impacts of multi-decadal climate variability may be greater than the impacts of climate change (Fig. 1). For this climate model and for these experiments, the impacts of climate change on mean runoff by 2050 are significantly greater than natural climate variability in northern and southern Europe, but are no different to those of natural climate variability across large parts of western and central Europe. Similar results were found using the value of the monthly runoff that was exceeded 90% of the time; this is a measure of low flow, calculated from the 30 individual years of simulated monthly runoff. This is because although the percentage impact of climate change on this extreme is greater than on the mean, the impact of multi-decadal natural climate variability on this measure is also greater. Different results may be obtained with other definitions of extreme behaviour; where an increase in mean precipitation is associated with a greater relative increase in precipitation intensity, for example, the flood signal might expect to be strengthened.

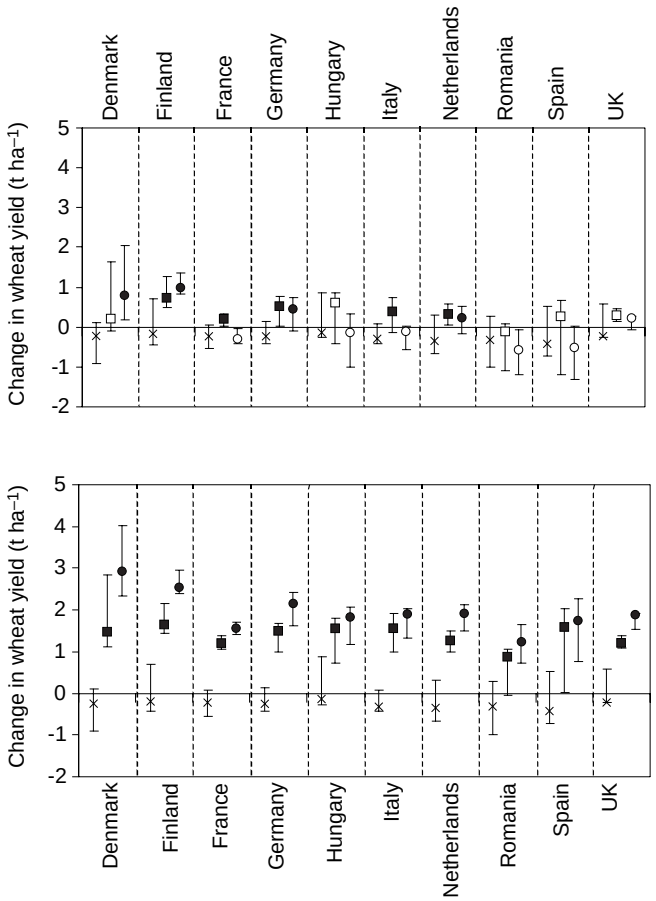

Figure 2 Relative changes in mean wheat yield at a national scale. Change in mean water-limited wheat yield (t ha^{-1} change from 1961–90 yield) for ten European countries due to natural climate variability (left bar; n=7) and due to climate and CO_2 change by 2050 under the GGd (middle bar; n=4) and GGa forcing scenarios (right bar; n=4). Top panel, atmospheric CO_2 concentration is held constant at 334 parts per million by volume (p.p.m.v.). Bottom panel, atmospheric CO_2 concentration increases to 435 p.p.m.v. for the GGd scenario and to 515 p.p.m.v. for the GGa scenario. Horizontal lines show maximum and minimum estimates in each case. Ensemble-median estimates are marked with an open square (GGd) or circle (GGa) where climate change causes a non-significant change in yield and with a filled square or circle where the change is significant at the 95% level from two-tailed t-test. Ensemble-median impacts are the median of the four impacts induced by the four ensemble-member climate changes.

Winter wheat yield was simulated at this same spatial resolution using the EuroWheat model[10]. EuroWheat is a simple mechanistic crop model that simulates the response of wheat development and yield to changes in climate (temperature, precipitation, solar radiation, relative humidity and wind speed) and atmospheric concentrations of carbon dioxide (through altered radiation use and water-use efficiencies). The model operates at two interacting time intervals: development and potential growth are determined on a daily time-step whilst water limitations to growth are computed on a monthly basis. EuroWheat has been shown to emulate the behaviour of widely used daily models (for example, AFRCWHEAT[20,21], CERES[22,23]) under current and future climates at two sites in Europe[10]. It is also able to reproduce well the observed spatial pattern of wheat yield and has been used to investigate climate-change impacts on European wheat productivity[10,24,25].

Wheat productivity in Europe is highly sensitive to multi-decadal natural climate variability, with local (that is, 0.5° grid cell) changes in 30-year mean water-limited yield of up to ± 3 t ha^{-1} (approximately $\pm$45% of mean 1961–90 yield). When wheat yields are aggregated to the national scale, the absolute range of yield response to climate variability decreases, but still varies from 0.5 t ha^{-1} (8% of mean 1961–90 yield) in Italy to 1.3 t ha^{-1} (14.6%) in Romania (Fig. 2, top panel). Climate change alone—without considering effects on the plant of elevated CO_2 concentrations—only results in significant changes (in this case increases) in mean yield by 2050 for both GGa and GGd scenarios in three northern European countries: Finland, Germany and the Netherlands (Fig. 2, top panel). Elsewhere in Europe, climate-change impacts on mean wheat yield are indistinguishable from those due to natural climate variability, although Denmark, France and Italy experience significant yield increases under at least one of the two forcing scenarios. Including the effects of elevated CO_2 alters the signal-to-noise ratio for wheat yield substantially (Fig. 2, bottom panel). Ensemble-median national yields increase by between 1.2 (15%) and 2.9 t ha^{-1} (39%) for the GGa scenario and between 0.9 (9%) and 1.8 t ha^{-1} (29%) for the GGd scenario. All these increases are statistically significant. This high sensitivity of wheat yield to CO_2 concentration has been reported in many experimental and modelling studies[26–28], although whether such increases would be fully realised in the field and at large scales is less clear.

We believe that this is the first use in climate-change impact analysis of climate model results extracted both from long simulations of unforced climate and from ensemble scenario simulations. Conventional impact analyses implicitly assume that each scenario represents just the signal of climate change and that multi-decadal natural climate variability can be ignored. Our analysis shows that these assumptions are not correct. First, there *is* considerable variability in unforced 30-year climates and this natural climate variability can induce non-trivial responses in impact indicators. This conclusion is strengthened given the likelihood that the climate model simulations used here have underestimated natural climate variability[29]. Second, climate-change scenarios derived from ensembles of climate model simulations, even when averaged over 30 years, contain differing magnitudes of both climate variability and climate change and this induces substantial uncertainty in the impact signal.

The particular patterns and magnitudes of change in runoff and wheat yield produced by our analysis may be specific to the climate and impact models used and to our choice of impact indicator (mean or extremes). Furthermore, the impact signal may be either over- or under-estimated, given that we have not simultaneously considered changes in variables such as land use, fertiliser application, pests, soil erosion or plant breeding. The way we interpret these changes, however, has wider validity and the results have a number of important general implications.

First, in some sectors and for some regions human-induced climate change may not have as great an impact on natural resources as might multi-decadal natural climate variability. Comparing present resources only with those simulated under future climate change may exaggerate the importance of climate change by ignoring the impacts of natural variability on these time-scales: the estimated impacts may occur even in the absence of human-induced climate change. Second, the results suggest that in many areas it will be very difficult to detect the impact of climate change, even on a multi-decadal time scale; the different spatial patterns of climate change and climate-variability impact, suggest that detection is best undertaken by looking over a large geographic area. Third, adapting our management systems to withstand multi-decadal natural climate variability (adequately defined) may, in some sectors and for some regions, be a sufficient medium-term response to the prospect of climate change—although elsewhere it may not. Last, the results do not suggest that we can ignore the possibility that climate change will affect our natural resource base; what they do show is that some impacts of natural climate variability may be as great as, or greater than, the estimated impacts of human-induced climate change. This study shows that it is possible, and suggests that it is important, to compare the impacts of climate change alongside those of natural multi-decadal climate variability in order both to assess the importance of climate change and to help in the development of appropriate adaptation strategies. □

Received 30 April; accepted 30 November 1998.

1. Parry, M. L., Carter, T. R. & Hulme, M. What is a dangerous climate change? *Glob. Environ. Change*, **6,** 1–6 (1996).
2. Wigley, T. M. L., Richels, R. & Edmonds, J. A. Economic and environmental choices in the stabilization of atmospheric CO_2 concentrations. *Nature* **379,** 240–243 (1996).
3. IPCC (eds Watson, R. T., Zinyowera, M. C., Moss, R. H. & Dokken, D. J.) *The Regional Impacts of Climate Change: an Assessment of Vulnerability* (Cambridge Univ. Press, 1998).
4. Kittel, T. G. F., Giorgi, F. & Meehl, G. A. Intercomparison of regional biases and doubled CO_2—sensitivity of coupled atmosphere–ocean general circulation model experiments. *Clim. Dyn.* **14,** 1–15 (1998).
5. Shugart, H. H. & Smith, T. M. A review of forest patch models and their applications to global change research. *Clim. Change* **34,** 131–153 (1996).
6. Dowlatabadi, H. Assessing the health impacts of climate change. *Clim. Change* **35,** 137–144 (1997).
7. Watson, R. T., Zinyowera, M. C. & Moss, R. H. (eds) *Climate Change 1995: Impacts, Adaptations and Mitigation of Climate Change: Scientific–Technical Analyses* (Cambridge Univ. Press, 1996).
8. Mitchell, J. F. B. & Johns, T. C. On the modification of global warming by sulphate aerosols. *J .Clim.* **10,** 245–267 (1997).
9. Arnell, N. W. The effect of climate change on hydrological regimes in Europe: a continental perspective. *Glob. Environ. Change* **9,** 5–23 (1999).
10. Harrison, P. A. & Butterfield, R. E. Effects of climate change on Europe-wide winter wheat and sunflower productivity. *Clim. Res.* **7,** 225–241 (1996).
11. Carter, T. R., Parry, M. L., Harasawa, H. & Nishioka, S. *IPCC Technical Guidelines for Assessing Climate Change Impacts and Adaptations* (UCL/CGER, London/Tsukuba, 1994).
12. Parry, M. L. & Carter, T. *Climate Impact and Adaptation Assessment* (Earthscan, London, 1998).
13. Hope, C., Anderson, J. & Wenman, P. Policy analysis of the greenhouse effect. *Energy Policy* **21,** 327–338 (1993).
14. Nordhaus, W. D. Optimal greenhouse gas reductions & tax policy in the 'DICE' model. *Am. Econ. Rev. Pap. Proc.* **83,** 313–317 (1993).
15. Fankhauser, S. *Valuing Climate Change* (Earthscan, London, 1995).
16. Tol, R. S. J. The damage costs of climate change: toward more comprehensive calculations. *Environ. Resource Econ.* **5,** 353–374 (1995).
17. Mitchell, J. F. B., Johns, T. C., Eagles, M., Ingram, W. J. & Davis, R. A. Towards the construction of climate change scenarios. *Clim. Change* (in the press).
18. Hulme, M. *et al.* Construction of a 1961–90 climatology for Europe for climate change impacts and modelling applications. *Int. J. Climatol.* **15,** 1333–1363 (1995).
19. Wilby, R. & Wigley, T. M. L. Downscaling general circulation model output: a review of methods and limitations. *Prog. Phys. Geogr.* **21,** 530–548 (1997).
20. Richie, J. & Otter, S. in *ARS Wheat Yield Project* (ed.Willis, W. O.) 159–175 (Dept of Agriculture, Agriculture Research Service, ARS-38, Washington DC, 1985).
21. Godwin, D., Ritchie, J., Singh, U. & Hunt, L. *A User's Guide to CERES-Wheat - V2.10* (Simulation manual IFDC-SM-2, Int. Fertilizer Development Center, Muscle Shoals, AL, 1990).
22. Weir, A. H., Bragg, P. L., Porter, J. R. & Rayner, J. H. A winter wheat crop simulation model without water or nutrient limitations. *J. Agric. Sci.* **102,** 371–382 (1984).
23. Porter, J. R. AFRCWHEAT2: a model of the growth and development of wheat incorporating responses to water and nitrogen *Eur. J. Agronomy* **2,** 69–82 (1993).
24. Harrison, P. A. Modelling the effects of climate change on wheat productivity in Europe. *Aspects Appl. Biol.* **45,** 41–48 (1996).
25. Harrison, P. A., Butterfield, R. E. & Gawith, M. J. in *Climate Change and Agriculture in Europe: Assessment of Impacts and Adaptations* (eds Harrison, P. A., Butterfield, R. E. & Downing, T. E.) 370–379 (Res. Rep. No. 9, Environmental Change Unit, Univ. Oxford, 1995).
26. Cure, J. D. & Acock, B. Crop responses to carbon dioxide doubling: a literature survey. *Agric. Forest Meteorol.* **38,** 127–145 (1986).
27. Kimball, B. A. *et al.* Productivity and water-use of winter wheat under free-air CO_2 enrichment. *Glob. Change Biol.* **1,** 429–442 (1995).
28. Batts, G. R. *et al.* Yield and partitioning in crops of contrasting cultivars of winter wheat in response to CO_2 and temperature in field studies using temperature gradient tunnels. *J. Agric. Sci.* **130,** 17–27 (1998).
29. Tett, S. F. B., Johns, T. C. & Mitchell, J. F. B. Global and regional variability in a coupled AOGCM. *Clim. Dyn.* **13,** 303–323 (1997).
30. Leggett, J., Pepper, W. J. & Swart, R. J. in *Climate Change 1992: the Supplementary Report to the IPCC Scientific Assessment* (eds Houghton, J. T., Callander, B. A. & Varney, S. K.) 75–95 (Cambridge Univ. Press, 1992).

Acknowledgements. Model data were obtained through the Climate Impacts LINK Project. This work was supported by DGXII of the Commission of the European Community.

Correspondence and requests for materials should be addressed to M.H. (e-mail: m.hulme@uea.ac.uk).

The origin of spinifex texture in komatiites

Mark Shore & Anthony D. Fowler

Ottawa-Carleton Geoscience Centre and Department of Earth Sciences, University of Ottawa, 140 Louis Pasteur, PO Box 450, Station A, Ottawa, Ontario K1N 6N5, Canada

Komatiites are high-temperature, fluid, magnesium-rich lavas typically of Archaean age. A striking characteristic feature of such lavas is 'spinifex' texture—plate-like crystals of olivine ($(Mg,Fe)_2SiO_4$), millimetres to decimetres long, in a fine-grained matrix of spherulitic clinopyroxene ($Ca(Mg,Fe,Al)(Si,Al)_2O_6$), dendritic chromite ($(Mg,Fe)(Cr,Al,Fe)_2O_4$) and altered glass[1–4]. Sheaves of olivine crystals can reach lengths exceeding one metre, even in komatiite flows less than 10 metres thick, in sharp contrast to the millimetre-scale post-eruption growth of crystals in more common volcanic rocks. Crystal growth of this magnitude might be a consequence of the high content of the constituent elements of olivine in komatiitic liquid, combined with the low viscosity and high chemical diffusivity of the lavas. But flows lacking spinifex texture are not uncommon, and those with such texture often contain substantial amounts of submillimetre olivine crystals of unremarkable appearance, so chemical considerations alone do not appear to provide a sufficient explanation. Here we present evidence that spinifex texture develops as a result of large thermal gradients, coupled with conductive and radiative heat transfer within olivine crystals fixed in the cool upper layers of the lava flows. This mode of growth has features in common with the high-temperature techniques used to grow large synthetic single crystals, but is rarely considered in geological contexts.

Many komatiites, including the exceptionally fresh and well exposed flows at Pyke hill in Munro township, northeastern Ontario, erupted as subaqueous lava flows[1,4]. The thermal effect of seawater infiltration into the fractured upper crust of the flows has not previously been considered in komatiite cooling models[5,6]. Thermal contraction of the solidified sheet-like lava flows (below ~1,000 °C) caused extensive fracturing on a centimetre to decimetre scale (Fig. 1). The permeability of a rock body can be estimated from the number and mean width of its fractures[7]; that of the illustrated Pyke hill lava tube is $\sim 10^{-11}\,m^{-2}$. This is close to the calculated bulk permeability of young oceanic crust ($\sim 10^{-12}\,m^{-2}$)[8]; by contrast, unfractured igneous rocks have typical *in situ* permeabilities of the order of 10^{-16} to $10^{-18}\,m^{-2}$. Thus we expect a substantial heat flux to have been transported by water circulation through cracks. Semiquantitative measurements of hydrothermal heat fluxes from basalt flows include $\sim 40\,kW\,m^{-2}$ at Heimaey[9], $100\,kW\,m^{-2}$ (with transient fluxes approaching $1\,MW\,m^{-2}$) at Kilauea[10], and $\sim 1\,MW\,m^{-2}$ at Vatnajökull[11] (estimated from data in that reference). Such heat transfer rates cannot be achieved by conduction through more than a few centimetres of solid rock. Because fracturing leads to further ingress of sea water, hydrothermal cooling/cracking fronts are probably self-propagating (at least in thin flows) and would migrate rapidly downwards. Observations[9–11] and modelling[12] of subaqueous basalt flows have demonstrated that cooling fronts could move at rates as high as several decimetres per hour, resulting in thermal gradients $>10^4\,K\,m^{-1}$ and